

Global H I profiles of spiral galaxies

J.J. Kamphuis, D. Sijbring and T.S. van Albada

Kapteyn Astronomical Institute, P.O. Box 800, NL-9700 AV Groningen, The Netherlands

received March 27, 1995; accepted September 4, 1995

Abstract. In this paper we present short H I synthesis observations of 57 galaxies without H I information in the RC3. These are a by-product of a large survey with the WSRT of the neutral hydrogen gas in spiral and irregular galaxies. Global profiles and related quantities are given for the 42 detected galaxies and upper limits for the remaining 15. A number of galaxies have low values of H I mass-to-blue luminosity ratio.

Key words: Catalogs; Galaxies: spiral; Radio lines: galaxies

1. Introduction

At the Kapteyn Institute a long-term project has recently been initiated to map neutral hydrogen gas (H I) in many hundreds of galaxies with the Westerbork Synthesis Radio Telescope (WSRT). This project, denoted as WHISP (Westerbork observations of neutral Hydrogen in Irregular and SPiral galaxies), will concentrate on nearby galaxies north of declination $\delta(1950) = 20^\circ$. Here we present the results of a side-product of WHISP: short observations of RC3 galaxies for which no H I data appear to be available. The main aim of these short observations is to determine the H I content. Observations of a few hours integration time are sufficient for that purpose. Below we present global profiles, and parameters derived from these, for 42 galaxies.

2. The sample

The sample from which WHISP candidates are being selected consists of galaxies in the Uppsala General Catalogue of Galaxies (UGC, Nilson 1973) with blue major diameters $d_b > 1.5$ arcmin and $\delta(1950) > 20^\circ$, 3148 in total. A subsample of 200 galaxies with $d_b > 2.0$ arcmin and flux densities at 21-cm larger than 200 mJy (as calculated from the ratio of total H I fluxes and profile widths

listed in the Third Reference Catalogue of Bright Galaxies (RC3, de Vaucouleurs et al. 1991)) presently serves as the main observing list for WHISP. Galaxies satisfying these selection criteria generally have redshifts less than 2000 km s⁻¹.

As a side-product of WHISP we present short observations of UGC galaxies, which obey the following criteria: $d_b > 1.5$ arcmin, $\delta(1950) > 20^\circ$, morphological type: S0 or later, $V_{\text{opt}} < 5000$ km s⁻¹, and without H I information in the RC3. The latter sample consists of 280 galaxies of which 57 have been observed.

3. Observations and data reduction

The observations have been carried out in the periods July - September 1992, August - September 1993 and December 1993 - February 1994 with the WSRT, using the Digital eXtended Backend (DXB) with 64 or 128 channels and with a total bandwidth of 1.25, 2.5 or 5 MHz; a uniform velocity taper has been used. The duration of the observations varies from two to six hours. The centre of the observed field lies within one arcmin of the optical position of the galaxy and the centre of the spectral passband is based on the redshift of the galaxy given in the RC3. A standard calibration is applied by observing 3C sources before and after the measurement of the galaxies.

The uv -data have been Fourier transformed, with a Gaussian taper of 390 meter (half-width), using the Dwingeloo reduction package NEWSTAR. A weighting proportional to the track length covered in the uv -plane has been applied and the uv -data have been convolved with an exponential sinc onto a rectangular grid. This results in channel maps which contain essentially one-dimensional information with an angular resolution of 60'' in the direction of the resolution axis, i.e. the projection of the E-W baseline onto the sky.

The reduction of the Fourier-transformed data has been carried out with the Groningen Image Processing SYstem (GIPSY, van der Hulst et al. 1992). We follow the method used by Warmels (1988). First, we have applied a Hanning smoothing in velocity to improve the sensitivity. Next, trial position-velocity (PV) maps along the resolu-

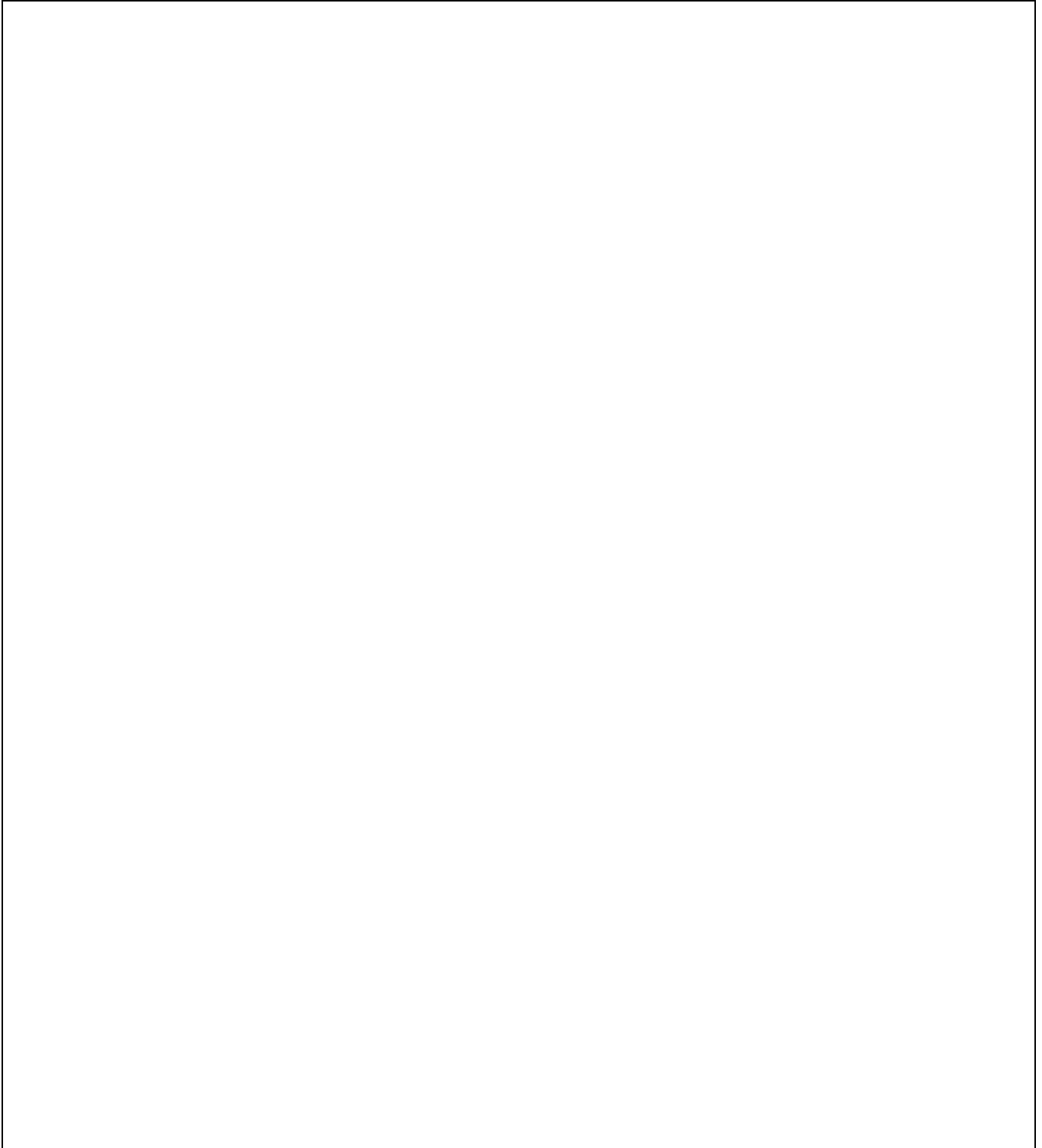


Fig. 1. Global H I profiles for 42 galaxies.



Fig. 1. Continued.

tion axis have been made using a range of sizes for the interval over which the signal is integrated in the direction perpendicular to the resolution axis. The continuum emission has been removed in the PV-maps by fitting a linear baseline in velocity to the signal in the channels free from HI emission, subtracting the result at all positions in the sky. The PV-map with the highest signal-to-noise ratio is then selected as the most appropriate map to derive the global HI properties of the galaxy. (Note that the PV-map has only been searched for HI emission near the position and redshift of the galaxy.) Due to the incom-

plete uv -coverage, the antenna pattern suffers from side-lobes with values up to 30 - 40% of the central peak, giving large depressions in the PV-map. We have suppressed these effects by CLEANing the map (Högbom 1974) with the corresponding antenna pattern, which is determined in the same way as the PV-map. The r.m.s. noise in the ‘cleaned’ PV-maps is typically 3 to 8 mJy/beam; a slightly varying zero-flux baseline is visible at a low level in some noisy profiles.

4. Global profiles

Because the spatial information on the galaxies is one-dimensional in a rather arbitrary direction we only derive the global profiles, i.e. the flux densities as a function of heliocentric radial velocity.

The shortest baseline is 36, 54 or 72 meter, implying that the observations are less sensitive to structures with sizes larger than 10, 7.5 and 5 arcmin, respectively. Assuming that the HI diameters are, on average, about a factor of two larger than the optical sizes, the HI sizes for the galaxies in our sample will typically be less than about 6 arc min. Therefore, the amount of HI emission missed in the global profiles will be small. Results for a comparison sample, consisting of galaxies with total HI fluxes known from single dish observations of which short WSRT observations have also been taken, indeed show that the total WSRT HI fluxes are within 10 percent of those derived from the single dish observations. This agrees with the findings of Warmels (1988), Oosterloo & Shostak (1993) and Broeils & van Woerden (1994).

The global profiles are shown in Figure 1; 42 out of 57 galaxies observed have been detected. The flux density at each radial velocity is determined as the sum of the flux in the CLEAN components and the flux in the residuals. Outside the velocity range of the HI emission the flux densities are set to zero. Several galaxies have an HI flux just above the detection limit, resulting in irregular, noisy profiles. A number of galaxies have profiles with peak flux densities in excess of 100 mJy.

From the global profiles we have derived the total HI mass, the profile width and the systemic velocity. The profile width is determined as the difference between the velocities at the low and high velocity sides of the profile, at the customary flux density levels of 20 and 50 percent of the peak value. Following the precepts of Sullivan et al. (1981), the uncertainty in the profile width is estimated by allowing the 20 and 50 percent flux density levels to vary within the r.m.s. noise of the profile. The systemic velocity is, in principle, determined as the error-weighted mean of the midpoints of the two velocities at the 20 and 50 percent flux density levels. Due to the low signal-to-noise ratio of several global profiles, the 20 percent level width, however, is often unreliable. Therefore, this flux density level has only been used in cases where the peak signal-to-noise ratio in the profile is larger than 15; otherwise the systemic velocity relies only on the 50 percent flux density level.

5. Sample properties

The sample of galaxies presented here is not complete in any magnitude or diameter-limited sense. Morphological types range from S0 to Im, with an over-abundance of Sb galaxies, and the absolute blue magnitudes range from -

22 to -14 ($H_0 = 75 \text{ km s}^{-1} \text{ Mpc}^{-1}$). Table 1 presents the main results; the meaning of the columns is as follows:

Column 1) UGC number.

Column 2) NGC or IC number.

Column 3) Spectral bandwidth of the observation. (Note that $2.5n$ MHz bandwidth at the 21-cm line rest frequency corresponds to $527n \text{ km s}^{-1}$.)

Column 4) Hanning tapered velocity resolution.

Column 5) Morphological type as given in the RC3.

Column 6) Inclination, determined as $\cos i = (q^2 - q_0^2)/(1 - q_0^2)$ where i is the inclination; q is the ratio of the observed minor and major axis sizes at the 25th blue magnitude isophote as given in the RC3. The intrinsic axial ratio q_0 of the disk has been taken from Guthrie (1992) (0.4 for type S0; 0.2 for types S0/a, Sa and Sab; 0.1 for type Sb; 0.15 for type Sbc; 0.1 for types Sc, Scd and Sd; 0.4 for types Sm and Im). For the types S?, a value of $q_0 = 0.2$ has been taken.

Column 7) Distance in Mpc, taking H_0 equal to $75 \text{ km s}^{-1} \text{ Mpc}^{-1}$ and correcting the heliocentric radial velocity for the motion of the Sun with respect to the centroid of the Local Group, using $(V_{\text{hel}} + 300 \sin l \cdot \cos b)/H_0$ (de Vaucouleurs et al. 1976); V_{hel} is the HI systemic velocity (cf. Column 13) or, if unavailable, the optical systemic velocity.

Column 8) Angular optical diameter at the 25th blue magnitude isophote as given in the RC3.

Column 9) Apparent blue magnitude as given in the RC3, corrected to a ‘face-on’ appearance, and corrected for Galactic and external extinction. If not given in the RC3, this quantity has been taken from the UGC and corrected according to the transformations in the RC3.

Column 10) Observed width of the global profile at the 50 percent level of the flux density peak. No widths are given for galaxies with poor global profiles. For widths at the 20 percent level, see note *c* to Table 1.

Column 11) Width of the global profile at a level of 50 percent of the flux density peak, corrected for inclination and for instrumental and turbulent broadening. The instrumental broadening has been determined using the precepts of Bottinelli et al. (1990). The correction for the turbulent motions has been derived using the prescriptions of Tully & Fouqué (1985). The value for the contribution by non-circular motion is taken as 14 km s^{-1} (Bottinelli et al. 1983).

Column 12) Optical heliocentric systemic velocity from the RC3.

Column 13) 21-cm heliocentric systemic velocity derived from the global HI profile.

Column 14) Integral of the global profile. The uncertainties are of the order 10 - 20 percent, but may be larger for profiles with low signal-to-noise ratio.

Column 15) Total HI mass, calculated as $M_{\text{HI}} = 2.36 \cdot 10^5 \cdot d^2 \cdot FI M_{\odot}$ (assuming that the HI is optically thin); d is the distance in Mpc and FI is the flux integral in Jy km s^{-1} . For the non-detections, listed at the bottom of Table

Table 1. Results of short WSRT observations for 57 UGC galaxies.

UGC	NGC/IC	B	ΔV	$Type$	i	d	D_{25}	B_T^0	W_{50}	W_{50}^i	V_{opt}	V_{HI}	FI	M_{HI}	M_{HI}/L_B	Notes
(1)	(2)	(MHz)	(km/s)	(5)	($^\circ$)	(Mpc)	(')	(mag)	(km/s)	(km/s)	(km/s)	(km/s)	(Jy km/s)	($10^9 M_\odot$)	($M_\odot/L_{B,\odot}$)	(17)
1034	N 551	5.0	34.1	Sbc	66	65.6	1.82	12.69			4901		4.9	4.97	0.09	a
1291	I 1731	2.5	8.4	Sc	51	44.8	1.55	13.45			3426		7.6	3.60	0.29	
1970		5.0	16.7	Scd	86	23.7	2.34	13.34	209 ± 7	193	1915	1914 ± 4	5.3	0.70	0.19	
2067		5.0	16.8	Sab	90	51.3	1.95	13.57	98 ± 8	87	3839	3885 ± 4	15.3	9.49	0.66	b
2069		2.5	8.4	Sd	54	49.9	2.34	12.54	257 ± 25	298	3715	3777 ± 12	17.7	10.4	0.30	
2392		5.0	16.7	Scd	77	21.4	1.86	13.50	148 ± 11	137	1548	1551 ± 6	6.0	0.65	0.24	
2526		5.0	34.1	Sb	80	66.1	3.55	11.67	589 ± 32	580	4996	4960 ± 16	6.9	7.13	0.05	
2548	N 1207	2.5	8.4	Sb	44	64.1	2.29	12.54			4787		5.8	5.63	0.10	
2617		2.5	8.4	Sd	70	63.7	2.51	12.48			4860		5.1	4.88	0.08	
2920		5.0	34.0	Scd	83	53.1	2.29	12.37	385 ± 22	369	4158	4151 ± 11	13.0	8.66	0.19	
3165		5.0	16.8	Im	61	51.6	2.29	14.6	101 ± 3	103	3780	3759 ± 1	16.2	10.2	1.73	c
3458		2.5	8.4	Sb	77	59.4	2.40	13.51			4292		3.4	2.83	0.14	
4271	N 2523	5.0	33.9	Sbc	53	47.6	2.95	12.07	448 ± 26	540	3415	3468 ± 13	12.8	6.84	0.14	d
4630	I 520	5.0	33.9	Sab	38	42.8	1.95	12.32			3528		4.0	1.73	0.05	
4705	N 2710	5.0	33.8	Sb	61	36.0	2.00	13.14	289 ± 13	309	2538	2508 ± 7	15.4	4.71	0.45	
4825	N 2748	5.0	16.7	Sbc	69	23.4	3.02	11.69	288 ± 6	291	1456	1476 ± 2	29.4	3.79	0.23	c
4906		5.0	33.8	Sa	79	32.2	2.00	12.89			2322		4.9	1.20	0.11	
6348	N 6348	5.0	16.7	Sb	72	25.1	2.00	13.19	235 ± 10	230	1966	1924 ± 5	15.4	2.30	0.47	
6458	N 3683	5.0	16.7	Sc	69	20.4	1.86	12.67	339 ± 32	346	1656	1722 ± 16	20.8	2.04	0.39	
7127	N 4133	5.0	16.7	Sb	42	16.5	1.82	12.78	289 ± 37	404	1296	1359 ± 18	8.0	0.52	0.17	
7290	N 4220	5.0	16.7	S0	90	14.2	3.89	12.23			979		6.2	0.29	0.08	
7329	N 4250	5.0	33.7	S0	42	24.9	2.69	12.70	152 ± 16	202	2032	2019 ± 6	19.4	2.84	0.38	c
7443	N 4314	5.0	16.7	Sa	28	12.5	4.17	11.21			963		1.1	0.04	0.01	
7714	N 4525	5.0	16.7	Scd	60	14.9	2.57	12.41	149 ± 9	156	1131	1172 ± 4	6.5	0.34	0.10	
7962	N 4693	5.0	16.7	Sd	80	23.7	2.46	12.98	256 ± 9	244	1647	1674 ± 5	14.1	1.86	0.35	
7994	N 4750	5.0	16.7	Sab	25	19.5	2.04	12.07	292 ± 22	660	1614	1618 ± 11	8.7	0.78	0.09	
8835	N 5362	5.0	33.8	Sb	64	29.0	2.29	12.70	296 ± 8	309	2232	2175 ± 4	9.4	1.86	0.18	
8935	N 5422	5.0	16.8	S0	90	24.3	3.89	12.79			1782		4.8	0.67	0.10	
8958	N 5443	5.0	16.7	Sb	69	24.1	2.69	12.52	408 ± 59	420	1921	1787 ± 29	5.9	0.81	0.10	
9115	N 5526	5.0	33.7	Sbc	90	29.1	1.78	14.5	200 ± 59	182	1971	2086 ± 29	8.1	1.62	0.85	
9428	N 5707	5.0	33.8	Sab	88	28.9	2.57	12.49	366 ± 24	348	2208	2191 ± 12	11.6	2.29	0.19	
9516	I 1056	2.5	8.4	Sb	45	53.3	1.82	13.76			4013		10.3	6.91	0.53	
9852	N 5929	5.0	33.8	Sb	59	32.7	1.66	13.0			2672		3.8	0.96	0.10	e
9948	N 5981	5.0	33.7	Sc	83	28.1	2.82	12.79			1764		0.9	0.17	0.02	
10437		5.0	33.7	S?	30	32.4	2.09	14.57	211 ± 11	385	2595	2602 ± 6	14.8	3.68	1.61	
10713		5.0	33.6	Sb	81	15.2	1.82	12.79	228 ± 38	212	1112	1074 ± 19	19.6	1.06	0.41	
10917	I 1265	5.0	16.7	Sab	67	24.9	2.04	13.45	271 ± 36	276	2161	2156 ± 18	6.8	0.99	0.26	
11432	N 6796	5.0	16.7	Sbc	79	28.1	1.86	12.26	442 ± 34	433	2090	2198 ± 17	13.2	2.47	0.17	
11466		5.0	33.6	S?	56	11.2	2.00	11.33	167 ± 7	181	782	818 ± 2	33.3	0.98	0.18	c
11470	N 6824	5.0	16.8	Sb	47	42.4	1.70	11.89			3337		4.6	1.95	0.04	
11635		2.5	8.4	Sbc	66	60.7	2.88	12.88			4731		6.0	5.22	0.14	
11920		5.0	33.6	S0/a	52	15.3	2.40	11.12			1145		5.3	0.29	0.02	
2521	N 1186	2.5	8.4	Sbc	69	37.0	3.16	10.89			2658			<1.13	<0.01	
3994	I 469	5.0	33.7	Sab	65	25.5	2.19	12.87			2080			<0.63	<0.09	
4544	N 2639	5.0	33.9	Sa	54	42.1	1.82	12.26			3198			<0.76	<0.02	
4645	N 2681	5.0	33.6	S0/a	25	10.4	3.63	10.90			683			<0.03	<0.01	
5568	N 3182	5.0	33.7	Sa	32	30.2	1.82	12.88			2130			<0.53	<0.06	
5692		5.0	16.6	Sm	66	2.7	3.24	13.24			180			<0.01	<0.03	
6392	N 3652	5.0	33.7	Scd	72	31.1	2.00	12.15			2096			<0.23	<0.01	
6484	N 3683A	5.0	33.8	Sc	44	28.5	2.34	12.38			2446			<0.27	<0.02	
7328	N 4245	5.0	16.7	S0/a	42	9.2	2.88	12.05			890			<0.04	<0.02	
7429	N 4319	5.0	16.7	Sab	40	23.3	2.95	12.55			1700			<0.32	<0.04	
7572	N 4441	5.0	16.7	S0	44	34.4	3.24	13.25			1466			<0.63	<0.07	
8722	N 5308	5.0	33.7	S0	90	27.5	3.72	12.43			2041			<0.42	<0.04	
9016	N 5475	5.0	16.7	Sa	80	22.2	2.04	12.88			1720			<0.41	<0.08	
10560	I 1231	2.5	8.5	Scd	63	67.8	2.19	13.07			5107			<2.70	<0.07	
10676		5.0	33.6	Im	70	9.7	1.82	15.9			524			<0.01	<0.17	

a. (UGC 1034) Possibly also HI emission at the edge of the spectral band.

b. (UGC 2067) The observed global profile is possibly that of the companion UGC 2065, a face-on Sm galaxy at 2.5 arcmin from UGC 2067.

c. W_{20} has been determined for four galaxies: UGC 3165: $141 (\pm 5)$ km s $^{-1}$; UGC 4825: $319 (\pm 8)$ km s $^{-1}$; UGC 7329: $236 (\pm 17)$ km s $^{-1}$; UGC 11466: $251 (\pm 7)$ km s $^{-1}$.

d. (UGC 4271) Arp 9.

e. (UGC 9852) Arp 90.

1, we estimate a 2σ upper limit for the HI mass, assuming typical values for the corrected profile widths for different morphological types (200 km s⁻¹ for types S0 to Sc; 120 km s⁻¹ for type Scd; 70 km s⁻¹ for type Sm; 50 km s⁻¹ for type Im).

Column 16) Total HI mass-to-blue luminosity ratio.

Column 17) Notes on individual galaxies.

6. Discussion

For the galaxies presented here, HI information in the RC3 is absent. As some of them are fairly large ($d_b > 3$ arcmin), we suspect that several galaxies may have been observed earlier but have not been detected. It is therefore of some interest to look at the HI content of the galaxies in our sample.



Fig. 2. HI mass-to-blue luminosity ratio versus morphological type. The solid line represents the mean value for the RC3-UGC sample from Roberts & Haynes (1994); the dashed lines are the 25 and 75 percentiles. The arrows indicate upper limits for the non-detections.

In Figure 2 we plot the HI mass-to-blue luminosity ratio versus morphological type. Arrows indicate upper limits. The solid line represents the mean relation, and the dashed lines 25 and 75 percentiles, as given by Roberts & Haynes (1994). The graph shows that the HI content is somewhat below the mean relation, especially for later types. A number of our upper limits are interestingly low: a factor of 20 below the mean. This indicates that we are now exploring the fainter part of the HI mass function. Apparently, for most galaxies in the RC3 with a high HI content an HI entry is available.

The Tully-Fisher relation (absolute blue magnitude versus corrected profile width) is shown in Figure 3. Except for UGC 2067 (whose measurement probably refers to the Sm galaxy UGC 2065), there is fair agreement with the mean relation given by Pierce & Tully (1992). Note that the three galaxies furthest below the line are close to face-on and their inclination corrected profile widths are therefore uncertain.

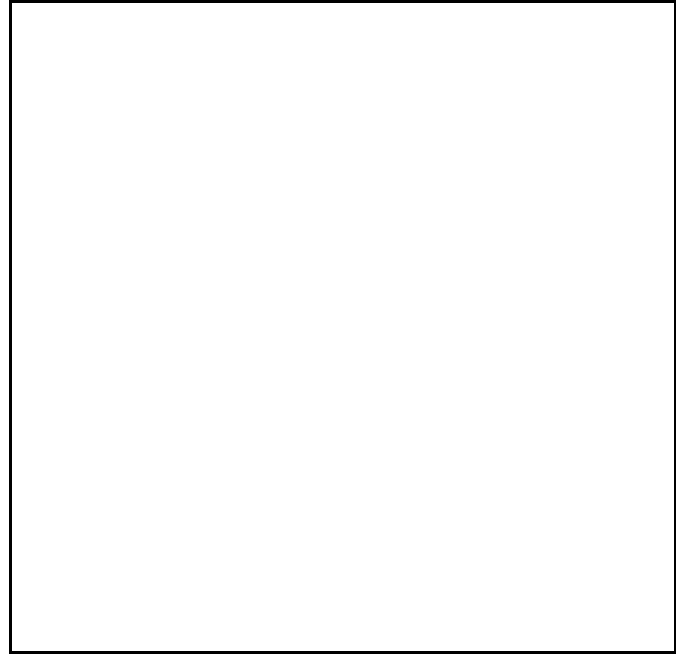


Fig. 3. Absolute blue magnitude versus profile width. The solid line is the Tully-Fisher relation as given by Pierce & Tully (1992, corrected to $H_0 = 75$ km s⁻¹ Mpc⁻¹). The measurement for UGC 2067 probably refers to the Sm galaxy UGC 2065 at 2.5 arcmin from UGC 2067.

Acknowledgements. The WSRT is operated by the Netherlands Foundation for Research in Astronomy with financial support from the Netherlands Organisation for Scientific Research (NWO). We thank J.M. van der Hulst and R. Sancisi for comments.

References

- Bottinelli, L., Gouguenheim, L., Paturel, G., de Vaucouleurs, G., 1983, *A&A*, 118, 4
- Bottinelli, L., Gouguenheim, L., Fouqué, P., Paturel, G., 1990, *A&AS*, 82, 391
- Broeils, A.H., van Woerden, H., 1994, *A&AS*, 107, 129
- Guthrie, B.N.G., 1992, *A&AS*, 93, 255
- Högbom, J.A., 1974, *A&AS*, 15, 417
- Hulst, van der, J.M., Terlouw, J.P., Begeman, K.G., Zwitzer, W., Roelfsema, P.R., 1992, *First Annual Conference on Astronomical Data Analysis Software and Systems*, Tucson, Arizona, eds. D.M. Worrall, C. Biemesderfer and J. Barnes, A.S.P. Conf. Series no. 25, p. 131

- Nilson, P., 1973, *Uppsala Astron. Obs. Ann.* **6** (UGC)
- Oosterloo, T.G., Shostak, G.S., 1993, *A&AS*, 99, 379
- Pierce, M.J., Tully, R.B., 1992, *ApJ*, 387, 47
- Roberts, M.S., Haynes, M.P., 1994, *A&AR*, 32, 115
- Sullivan, W.T. III, Bothun, G.D., Bates, B., 1981, *AJ*, 86, 919
- Tully, R.B., Fouqué, P., 1985, *ApJS*, 58, 67
- de Vaucouleurs, G., de Vaucouleurs, A., Corwin, H.G., 1976, *Second Reference Catalogue of Bright Galaxies* (Austin: University of Texas Press)
- de Vaucouleurs, G., de Vaucouleurs, A., Corwin, H.G., Buta, R.J., Paturel, G., Fouqué, P., 1991, *Third Reference Catalogue of Bright Galaxies* (New York: Springer-Verlag) (RC3)
- Warmels, R.H., 1988, *A&AS*, 72, 57